Hindawi
Advances in Polymer Technology
Volume 2022, Article ID 1866280, 16 pages
https://doi.org/10.1155/2022/1866280

Research Article

Synthesis, Characterizations, and Thermochromic Properties of VO_2 Particles Grafted with PSS:PEDOT

Onruthai Srirodpai,[1] **Jatuphorn Wootthikanokkhan**,[1] **and Saiwan Nawalertpanya**[2]

[1]*Materials Technology Program, School of Energy, Environment and Materials, King Mongkut's University of Technology Thonburi (KMUTT), Bangkok 10140, Thailand*
[2]*Department of Chemical Engineering, Faculty of Engineering, King Mongkut's University of Technology Thonburi (KMUTT), Bangkok 10140, Thailand*

Correspondence should be addressed to Jatuphorn Wootthikanokkhan; jatuphorn.woo@kmutt.ac.th

Received 1 April 2022; Revised 30 June 2022; Accepted 26 July 2022; Published 1 September 2022

Academic Editor: Kinga Pielichowska

Vanadium dioxide (VO_2) particles were modified by grafting with poly(styrene sulfonate) (PSS) and poly(3,4-ethylenedioxythiophene) (PEDOT) via surface-initiated atom transfer radical polymerization (SI-ATRP). Critical transition temperature (T_c) of the modified VO_2 ranging between 77 and 79°C was obtained. After mixing with acrylic-based emulsion, dispersion of the VO_2 particles in the polymer matrix was significantly improved. The visible light transmittance through the composite films above 75% was maintained if a concentration of the modified VO_2 particles loaded into acrylic polymer film was no greater than 1.0 wt%. The NIR transmittance through the acrylic/VO_2@PSS : PEDOT also dropped by 9-10%, compared with that of the pure acrylic film (without any particles). Finally, glass substrates coated with the acrylic/VO_2@PSS : PEDOT composite films could reduce the temperature inside a model house by 5-6°C, compared with that of the control system (pure acrylic coating film without VO_2 particles). Overall, this work demonstrated that it was possible to improve the dispersion of VO_2 particles in polymer films without sacrificing its NIR shielding ability by grafting the surface of VO_2 particles with PSS : PEDOT chains, while providing the optimum grafting density and particle loading.

1. Introduction

Vanadium dioxide, particularly that in the form of monoclinic crystal structure (VO_2(M)), is one of the most interesting types of thermochromic materials. This is because the critical phase transition temperature (T_c, 68°C) [1] of VO_2 is the lowest, compared to those of other thermochromic materials [2]. The transition temperature of VO_2 can also be further reduced by doping it with chemicals such as molybdenum (Mo) [3], niobium (Nb) [4], fluorine [5], and tungsten [1]. At a temperature above T_c, VO_2(M) is transformed into a tetragonal/rutile phase, accompanied with a decrease in spectral transmittance in the near infrared (NIR) region [6, 7]. Considering this interesting behavior, the feasibility of utilizing VO_2 as a coating layer on glass to enhance the energy efficiency in buildings has been explored. Practically, thin films of VO_2 can be coated onto glass substrates by several techniques including sputtering [8], chemical vapor deposition (CVD) [9], pulsed-laser deposition [10], and ion implantation technique [11]. However, these techniques usually require complex and expensive equipment. Alternatively, if the VO_2 material can be prepared in the form of particles, it is possible to develop polymer/VO_2 composite [1, 12–15], which can be further applied onto glass substrates by less complex techniques such as spray coating [16] and lamination [1, 12].

Despite the above advantages, some challenges have yet to be resolved. These include the fact that the NIR shielding efficacy of the $V5O_2$-based film is usually achieved at the expense of its optical transparency [6, 7]. This is related to the poor dispersion of VO_2 particles in many polymer matrices [17]. In this regard, surface modification

of VO_2 particles was undertaken to deal with the above problem.

Synthetic routes and structure-property relationships of polymer-grafted nanoparticles have been reviewed by Kumar and coworkers [18]. Efficacy of the grafted nanoparticles, for the enhancements of mechanical and optical properties of polymer nanocomposites, depends on many factors including the grafting density (σ), length of the grafting chains (N), length of the matrix chains (P), and the P/N ratio (α). Besides, the roles of size and shape of nanoparticles upon *crossover* of polymer chains and properties of the nanocomposites also deserve a consideration and have yet to be clarified.

Few studies concerning the surface modification of VO_2 particles have been reported in the open literature; however, all those works focus on the improvement of oxidation stability and the enhancement of photocatalytic activity of the materials [13–17, 19, 20]. For example, by coating the VO_2 particles with a polyethylene (PE) layer, the stability of the VO_2@PE particles against oxidation improved while the thermochromic behavior of the metal oxides was still maintained. Li et al. [19] prepared one type of core-shell VO_2@TiO_2 nanoparticles and reported that the chemical stability was enhanced by the TiO_2 shell. After carrying out the surface modification, the transmittance values (T_{lum} and ΔT_{sol}) of the VO_2 particles increased from 7.35% and 6.93% to 27.46% and 17.63%, respectively.

However, enhancing the NIR shielding property of VO_2-based film without sacrificing its optical transparency remains a challenge. In this study, it was proposed that if the VO_2 particles were grafted with a kind of special material, which is intrinsically transparent in the visible light region but capable of blocking the transmission of NIR radiation, the above challenging problems should be resolved. One possible candidate material for such a demanding condition includes poly(3,4-ethylenedioxythiophene) (PEDOT) whose heat shielding efficacy is known [21–24]. However, PEDOT is insoluble in water and many common organic solvents. In this regard, poly(styrene sulfonate) (PSS) was introduced into the PEDOT system to balance the polarity, dispersibility, and solubility of the polymer. Im et al. [22], for example, solved this problem by applying a copolymer, synthesized from styrene and sulfonated styrene (P(SS-co-St)) as a template for an oxidative polymerization of EDOT. By properly controlling the thickness of the P(SS-co-St) film, percentages of NIR shielding and visible light transmittance of 92 and 40 were achieved, respectively. Moreover, PEDOT:PSS-based materials in different configurations such as WO_3/PEDOT:PSS composite for electrochromic glass [24] and PEDOT:PSS/SWCNT composite for smart window applications [23] have also been developed and reported. To the best of our knowledge, however, the hybrid materials based on a combination of VO_2 particles and PEDOT:PSS have not been explored. In this study, it was hypothesized that by properly grafting the PEDOT:PSS chains onto the VO_2 particles, a steric hindrance imposed by the presence of PEDOT:PSS chains could be introduced and that could lead to better dispersion of the modified VO_2 (so called VO_2@PEDOT:PSS herein) particles in polymer matrices. This means that the NIR shielding property of VO_2-based film might be enhanced without sacrificing its optical transparency. Therefore, the aim of this work was to investigate the effects of composition and concentration of VO_2@PEDOT:PSS particles on morphological, thermal, and optical properties of the acrylic polymer films, reinforced with the VO_2-based particles.

2. Experiment

2.1. Materials. Vanadium pentoxide (V_2O_5, >98% pure), (3-aminopropyl) triethoxysilane (APTES, >99% purity), N,N,N′,N′-pentamethyldiethylenetriamine (PMDTA, 99%), copper (I) bromide (CuBr, >99% purity), α-bromoisobutyryl bromide (BIBB, $C_4H_6Br_2O$, >99% purity), and sodium 4-vinylbenzenesulfonated (SSNa, $C_8H_7NaO_3S$, ≥90% purity) were obtained from Sigma-Aldrich Co., Ltd. Citric acid (>99% purity) and methanol (99.8%) were obtained from Loba Chemie Pvt. Ltd. Toluene (analytical grade), chloroform (analytical grade), and ethanol (analytical grade) were obtained from Merck Co., Ltd. Triethylamine (TEA, >99% purity), 2,2′-bipyridyl (Bpy, >99% purity), and 3,4-ethylenedioxythiophene (EDOT, >98% purity) were obtained from TCI group Co., Ltd. An acrylic-based emulsion (PLIOTEC HDT 12 from Synthomer), used as a binder for preparing polymer/VO_2 composite films, was supplied by the RPSC Chemicals Co. Ltd. All chemicals were used without further purification.

2.2. Synthesis of VO₂@PEDOT:PSS Particles. PEDOT and PSS chains were sequentially grafted onto VO_2 particles through a "grafting from" approach via a surface-initiated atom transfer radical polymerization (SI-ATRP) mechanism. A schematic diagram, illustrating the chemical structures and synthetic route for preparation of PEDOT:PSS-grafted VO_2 (designated as VO_2@PEDOT:PSS), was proposed and is shown in Figure 1.

Basically, the synthesis is divided into 5 steps, as briefly described below. Firstly, a monoclinic phase VO_2 particles were prepared via hydrothermal and calcination techniques using vanadium pentoxide (V_2O_5) and citric acid ($C_6H_8O_7$) as raw materials and reducing agent, respectively. More details concerning the reaction conditions and procedures for these have been well described in our previous report [1]. After that, the VO_2 particles were grafted with the silane coupling agent (APTES) to introduce amine functional groups onto the surface of VO_2 particles. Again, more details concerning this reaction step have been reported elsewhere [25]. Next, α-bromoisobutyryl bromide (BIBB), which served as an initiating species for ATRP, was anchored onto the VO_2@APETS particles. The reaction was proceeded via a condensation between the amine groups of APTES moieties and the acyl-bromide group of BIBB. After that, PSS chains were grafted from the surface of VO_2 particles via a SI-ATRP of sodium styrene sulfonate (SS-Na). The polymerization was carried out under different reaction times, ranging from 12 to 24 h. Accordingly, the polymerized products (polystyrene sulfonate-grafted VO_2 particles) were designated as VO_2@PSS-12,

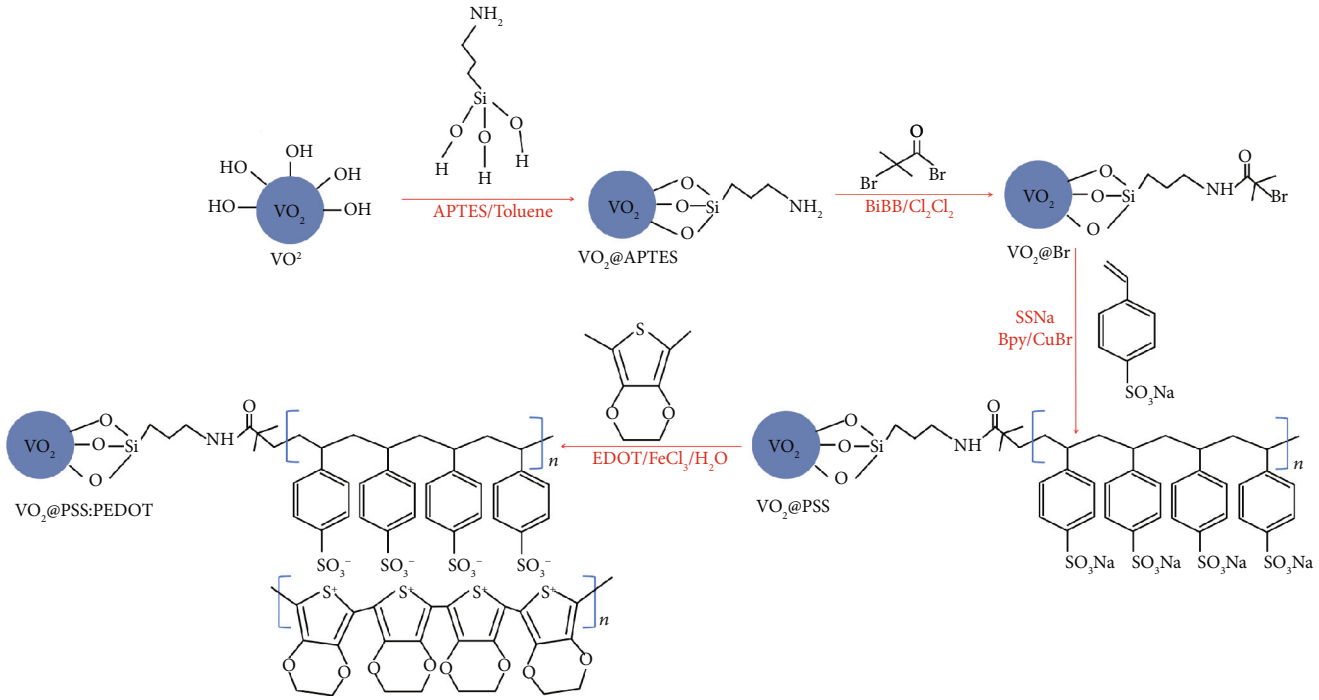

Figure 1: Schematic illustration of surface grafting of VO_2 particles with PEDOT: PSS chains.

Table 1: List of abbreviation for the sample names.

Sample name	Descriptions
VO_2	The neat vanadium dioxide particles, synthesized via hydrothermal and calcination techniques
VO_2@PSS-*xx*	VO_2 particles grafted with poly(styrene sulfonate) (where *xx* refer to the ATRP polymerization time)
VO_2@PSS : PEDOT	VO_2@PSS particles which were *in situ* mixed with poly(3,4-ethylenedioxythiophene)
PSS	Poly(styrene sulfonate)
PSS : PEDOT	Poly(styrene sulfonate) *in situ* mixed with poly(3,4-ethylenedioxythiophene)
VO_2@PE	VO_2 particles coated with a polyethylene layer

VO_2@PSS-16, VO_2@PSS-20, and VO_2@PSS-24, respectively (see Table 1).

Finally, EDOT monomer was polymerized on the surface of VO_2@PSS particles via an oxidative polymerization mechanism, utilizing the PSS shell layer as a dopant and template for the reaction. Likewise, the final products (VO_2 particles grafted with PSS : PEDOT) were designated as VO_2@PSS : PEDOT-12, VO_2@PSS : PEDOT-16, VO_2@PSS : PEDOT-20, and VO_2@PSS : PEDOT-24, respectively. More details regarding the synthesis of these particles are fully described in the supplementary information file (available here).

2.3. Preparation of Polymer/VO_2 Composite Films. To prepare the polymer/VO_2 composite films, different types of VO_2-based particles, including the neat VO_2, the VO_2@PSS : PEDOT-12, and the VO_2@PSS : PEDOT-24 were mixed with an acrylic-based emulsion. Depending on the concentration of particles to be loaded, a given amount of VO_2 particles (0.03 g, 0.06 and 0.09 g) were dispersed in 15 g of the acrylic emulsion (PLIOTEC HDT 12) in a beaker and then placed in an ultrasonic bath and kept stirred for 150 min. The above mixtures were then coated onto a glass substrate ($10 \times 10\ cm^2$) by using a bar coater. The final film thickness was controlled by selecting a suitable rod bar (with a specified gap between the rod and substrate of 80 nm). The coating was left overnight to allow complete drying.

2.4. Characterizations. Changes in chemical functional groups on the surface of the VO_2 particles were monitored by using Fourier transform infrared spectroscopy (FTIR, Thermo, DSC-1) and the X-ray photoelectron spectroscopy (XPS, AXIS ultra DLD), equipped with Avantage Data System software. The XPS data were collected in the V_{2p}, O_{1s} C_{1s}, N_{1s} S_{2p}, and Si_{2p} binding energy regions.

Crystal structures of the modified VO_2 particles were examined by using an X-ray diffractometer (XRD, Bruker AXS D8-Discover) in the 2θ range of 10–80°, using Cu-Kα radiation ($\lambda = 1.54178$ Å). The accelerating voltage and the current used were 40 kV and 40 mA, respectively. Thermogravimetric analysis (NETZSCH, TGA 209 model) was used to determine thermal stability and weight composition of the

VO_2-based particles. For TGA measurement, approximately, 8 mg of each sample was used and was scanned over temperatures ranging between 25°C and 800°C under nitrogen gas and a heating rate of 10°C/min. From the obtained TGA thermograms, grafting density (δ) of the final product (VO_2@PSS : PEDOT particles) was determined, using equation (1), which was adapted from the work of Babu and Raghavachari [26]

$$\left\lfloor \frac{(W_{200-800}/(100 - W_{200-800})) - W_{VO_2}}{MS100} \right\rfloor \times 10^6 \mu\text{mol/m}^2 \Bigg\rfloor, \quad (1)$$

where δ is the grafting density, $W_{200-800}$ is the percentage weight loss of polymer chains in the grafted VO_2, S is the surface area of VO_2 particles determined by BET technique (15.9887 m^2/g), W_{VO_2} is the percentage weight loss of VO_2 particles before grafting, and M is the molar mass of the immobilized molecules (the grafting chains).

In addition, thermal behaviors of VO_2 particles and polymer/VO_2 composites were investigated by differential scanning calorimetry, using DSC 204, NETZSCH instrument. Typically, about 8 mg of the sample was used and the specimens were scanned over temperatures ranging between 25°C and 800°C, under nitrogen gas atmosphere, at a heating rate of 10°C/min.

The morphology of VO_2 particles and the acrylic/VO_2 composite films were examined by using the scanning electron microscopy (SEM) and the transmission electron microscopy (TEM) techniques. The TEM experiment was carried out by using a JEOL JEM-2100 (JEOL, Peabody) microscope with an accelerating voltage of 200 kV. The TEM specimen was prepared by dispersing 1 mg of the VO_2 particles in 10 ml of ethanol, followed by sonication for 30 min. The solution was then dropped onto a copper grid and dried at 60°C. The SEM experiment was carried out by using a JEOL (JSM 6610LV) machine, equipped with a secondary electron detector and energy-dispersive X-ray detector (EDX). The accelerating voltage used was 10-30 kV. The sample was coated with gold prior to carrying out the SEM experiment.

Size of the VO_2-based particles was analyzed by using SEM and dynamic light scattering (DLS) techniques, respectively. The DLS analysis was carried out by using a Zetasizer instrument (Nano-ZS90, Malvern, UK), at a measurement angle 173 backscatter (NIBS default). The samples were prepared by dilution and sonication of the sample in an aqueous solution before putting into disposable cuvettes. The average hydrodynamic diameter was determined by taking an average of 11 runs, and the duration for each run was 10 sec. Each analysis is the average of results from three consecutive measurements.

Optical properties of the acrylic binder films, containing different types and concentration of VO_2-based particles, were tested by using a UV/visible/NIR spectrophotometer (Shimadzu, UV-3100). The percentage of light transmittance and reflectance of the 2×2 cm^2 film samples in the wavelength ranging between 200 and 2500 nm was investigated and calculated in accordance with the ISO 9050 standard method.

Heat shielding ability of polymer composite films containing VO_2 particles was tested by using a model house, equipped with an infrared lamp, thermocouples, and glass windows. More details concerning the experimental setup of this equipment has already been described in our earlier report [1]. Changes of temperature inside the house chamber was then monitored and followed as a function of time and the types of polymer/VO_2 window films.

3. Result and Discussion

3.1. Structural Characterizations of VO_2 Particles. Figure 2 shows overlaid FT-IR spectra of the various types of VO_2 particles, including the neat VO_2, the VO_2@APTES, VO_2@Br, VO_2@PSS, and VO_2@PSS : PEDOT. A broad absorption band centered around wavenumbers ranging between 3200 cm^{-1} and 3600 cm^{-1} and a sharp absorption peak at 1630 cm^{-1} can be noted from all spectra. These bands are assigned to the stretching vibration of hydroxyl groups (OH) on the VO_2 particles and the bending vibration of H-O bonds from the absorbed moisture, respectively [27–29]. After grafting with APTES, an intensity of a broad absorption band ranging between 3350 and 3650 cm^{-1}increased significantly. This can be ascribed to N-H stretching of NH_2 group in the APTES [30]. New peaks at 1400cm^{-1}, 1100 cm^{-1}, and 984 cm^{-1} also emerged (sample (b) in Figure 2). These are attributed to the vibration of the Si-CH_2 bond, the asymmetric stretching of the Si-O bond, and the stretching of the Si-OH bond, respectively.

To verify the existence of BIBB moieties on the surface of modified VO_2 particles (VO_2@Br), in this study, an XPS technique was used. From Figure 3, the presence of characteristic peaks in the XPS spectra at the binding energy of 68.25 eV and 182 eV was noted. These can be ascribed to the Br 3d and Br 3p orbitals, respectively. [31] The C 1s peak in the XPS spectrum was further analyzed by deconvolution. From Figure 4(a), the presence of a deconvoluted peak at 287.6 eV, representing the O=C-N group [5], can be noted. This indicates that the VO_2@APTES particles were successfully grafted with the BIBB initiator via an amide linkage.

The BIBB moieties on the surface of these particles were then used as an initiator for the polymerization of the sodium styrene sulfonate (SSNa) monomer. From FTIR analysis, the absorption peaks at 1175 cm^{-1} and 1038 cm^{-1}, which are attributed to asymmetric and symmetric stretching vibration of the SO_3 groups in the monomer [24, 32], were observed, respectively (see the inset in Figure 2). Moreover, from the XPS spectrum of this product (sample (b) in Figure 3), peaks at 167.5 eV and 1070.5 eV, which represent the binding energy of the S 2p and Na 1s orbitals, can be noted. The intensity of the C 1s peak at the binding energy 284.5 eV also increased. This indicates that the surface of the modified VO_2 particles was covered with more hydrocarbon component. In Figure 4(b), four deconvoluted peaks at the binding energy of 284.6 eV, 285.5 eV, 286.4 eV, and 287.6 eV were also noted. These can be assigned to C=C, C-C/C-H, C-O/C-S, and C=O/C=S bonds, respectively. In

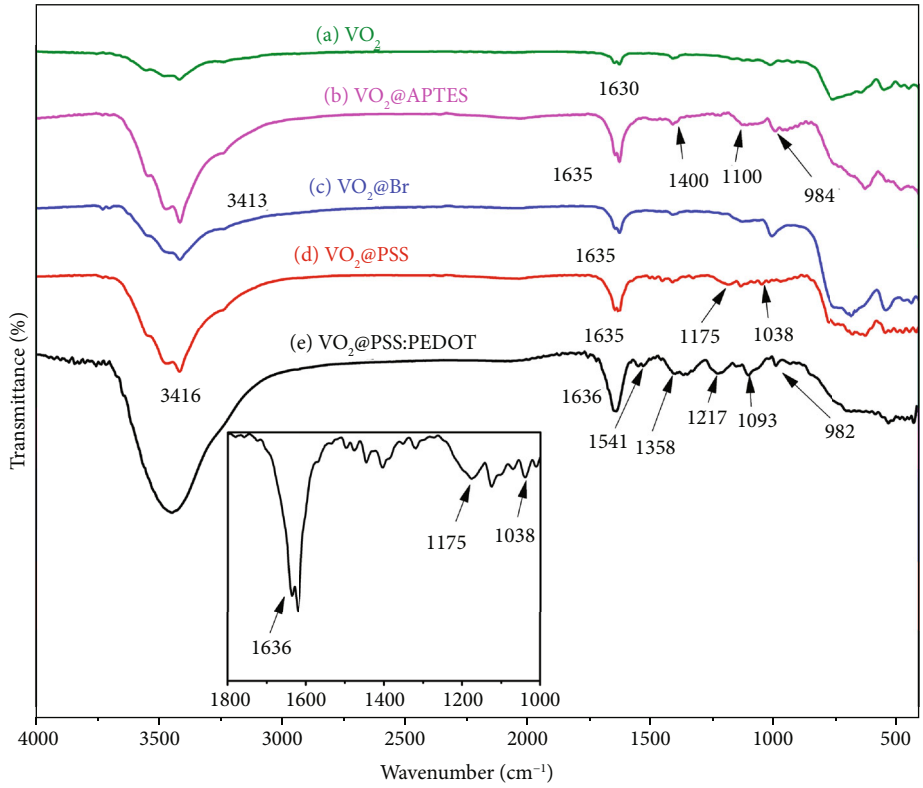

FIGURE 2: FT-IR spectra of various VO_2-based particles: (a) the neat VO_2, (b) VO_2@APTES, (c) VO_2@Br, (d) VO_2@PSS, and (e) VO_2@PSS : PEDOT.

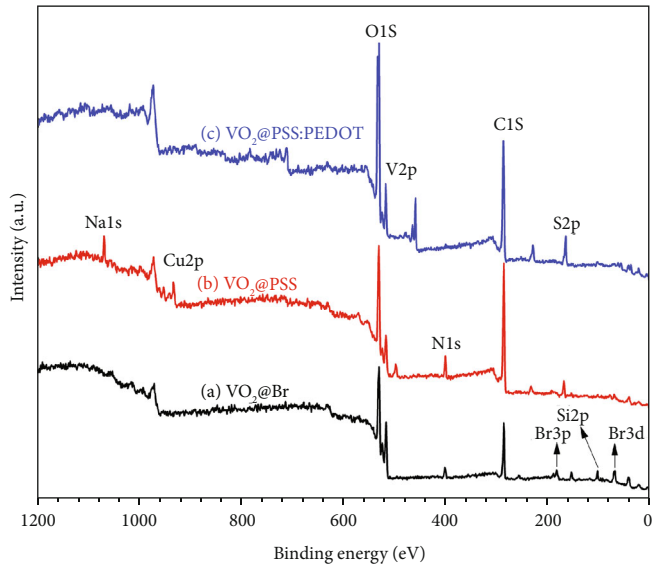

FIGURE 3: XPS survey spectrum of (a) VO_2@Br, (b) VO_2@PSS, and (c) VO_2@PSS : PEDOT particles.

addition, direct evidence supporting the presence of a PSS amorphous organic layer on the surface of the modified VO_2 particles can be seen from the TEM images of the products (Figure 5). The above results confirm that the monomer was successfully grafted on the VO_2 particles.

Finally, after reacting the VO_2@PSS particles with the EDOT monomer, the FTIR spectrum of the final product (VO_2@PSS : PEDOT) (sample (e) in Figure 2) shows additional absorption peaks at 1541 cm^{-1}, corresponding to C=C stretching of the thiophene rings in the PEDOT repeating units. Absorption peaks at 1358 cm^{-1} (C-C stretching of SO_3H), 1217 cm^{-1}, 1093 cm^{-1} (C-O-C stretching), and 982 cm^{-1} (C-S stretching) representing the PSS chains were also noted [4]. Consideration of the XPS spectra

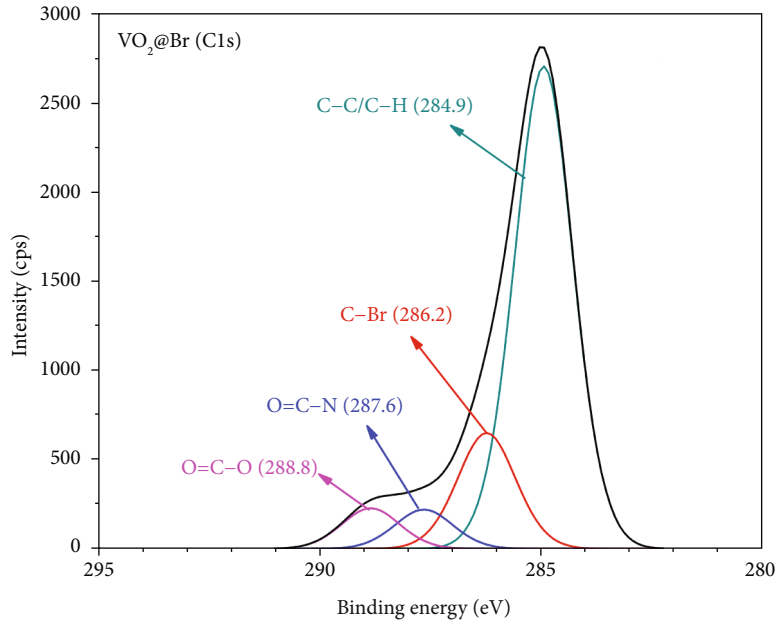

(a)

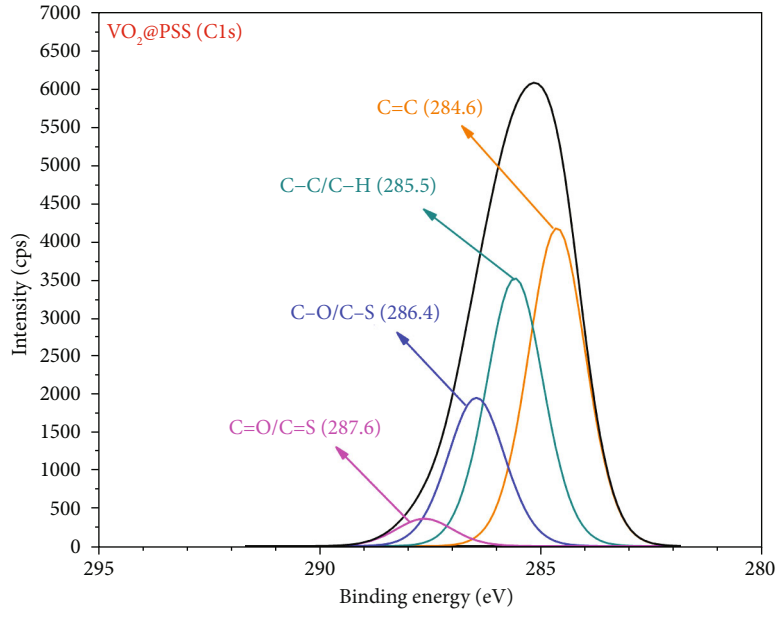

(b)

Figure 4: Continued.

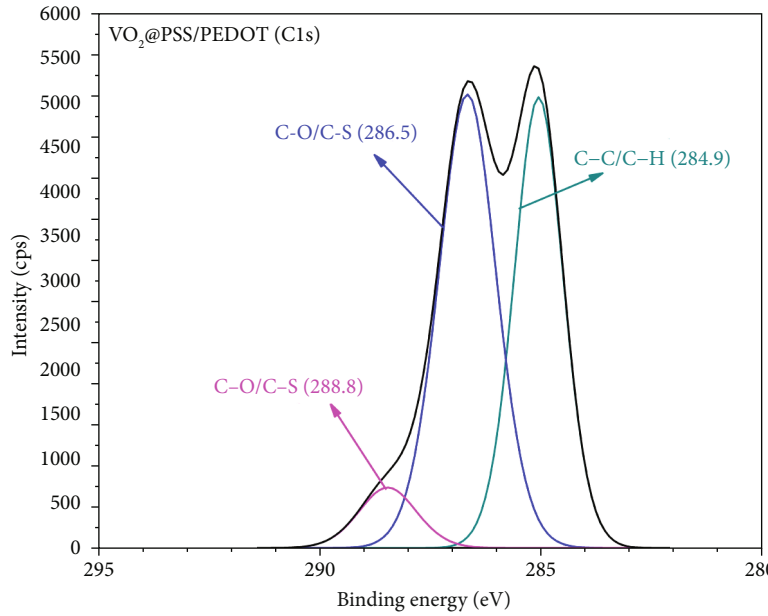

(c)

Figure 4: Peak fitting of C 1s of (a) VO_2@Br, (b) VO_2@PSS, and (c) VO_2@PSS : PEDOT particles.

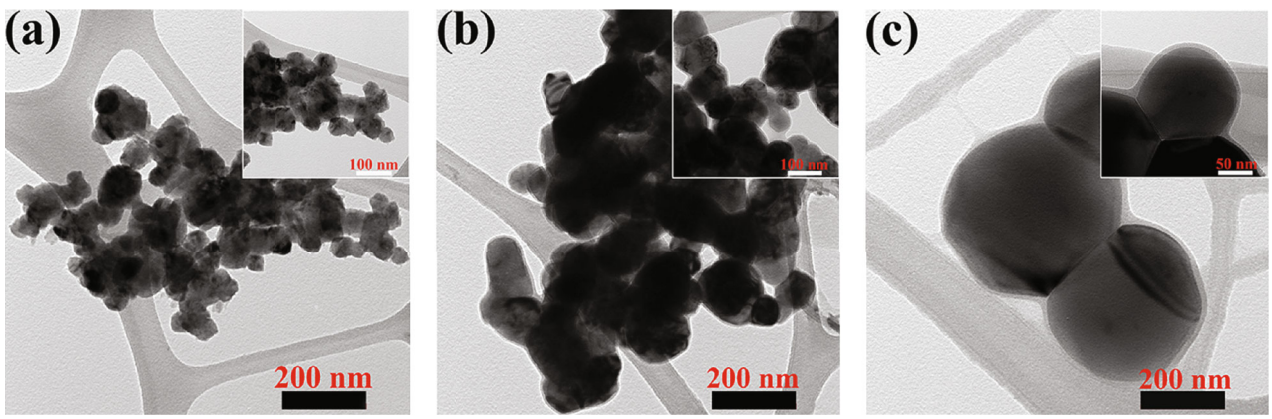

Figure 5: TEM images of (a) the neat VO_2, (b) VO_2@PSS-12, and (c) VO_2@PSS-24.

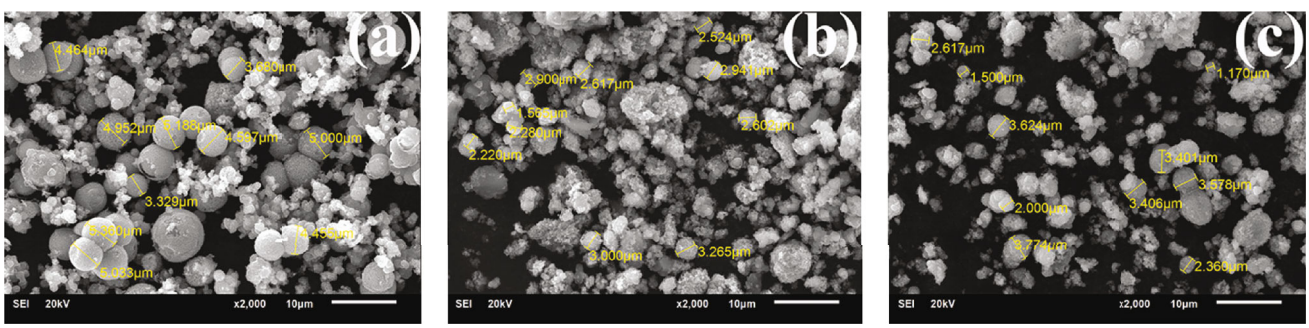

Figure 6: SEM images of VO_2 (a), VO_2@PSS-12 (b), and VO_2@PSS-24 (c) particles.

(Figure 4(c)) shows that the intensity of the deconvoluted XPS peaks (C-O/C-S and C=O/C=S bonds) increased after grafting with the EDOT. This suggests that the monomer was polymerized on the surface of the VO_2 particles via the PSS shell, which served as both a template and a dopant.

Figure 6 shows SEM images of VO_2-based particles. The particles are in a spherical shape, and sizes of the individual

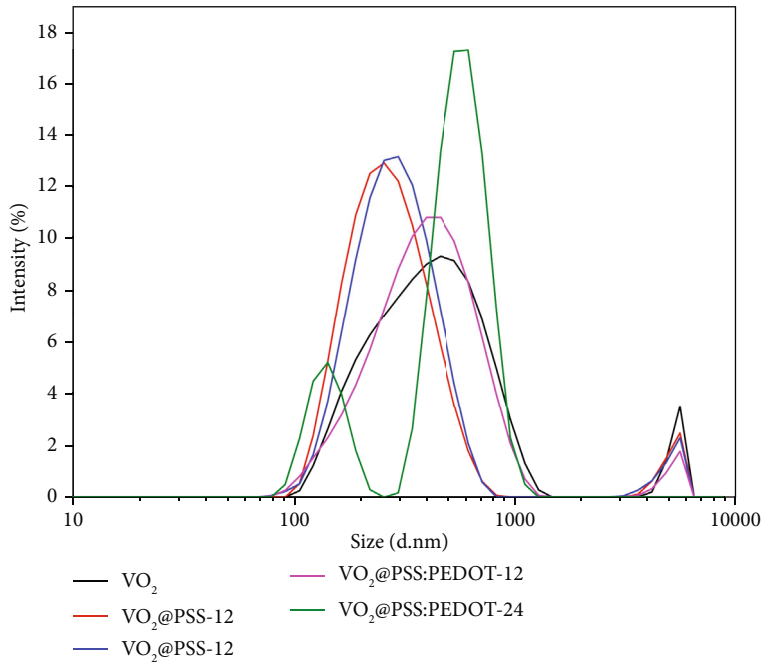

Figure 7: DLS intensity size distribution curves for VO_2-based particles.

Table 2: Parameters from DLS analysis of VO_2-based particles.

Materials	Particle size			
	Major peak		Minor peak	
	Range (nm)	D_h (nm)*	Range (nm)	D_h (nm)
VO_2	100-1000	475	4000-6500	5245
VO_2@PSS-12	100-900	280	3000-6500	5083
VO_2@PSS-24	70-900	295	3000-6500	5385
VO_2@PSS : PEDOT-12	70-1050	436	100-900	5025
VO_2@PSS : PEDOT-24	250-1050	563	70-250	149

*The values of D_h are corresponding to the peak positions on DLS intensity size distribution curves.

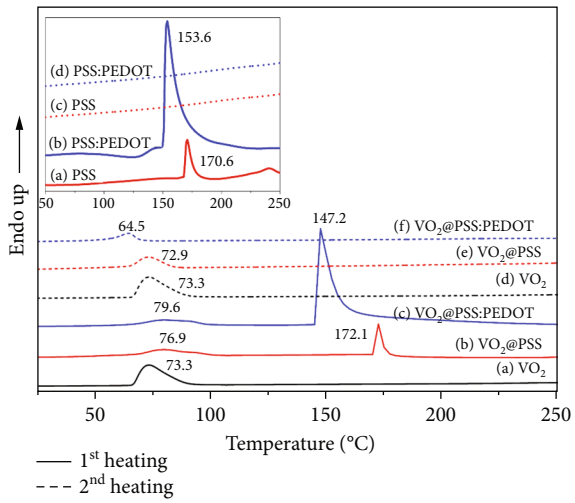

Figure 8: DSC thermograms of various VO_2-based particles: (a) the neat VO_2, (b) VO_2@PSS, and (c) VO_2@PSS : PEDOT; note that the dot lines represent the second heating thermograms for each sample.

Table 3: The critical transition temperature (T_c) and grafting density values of VO_2 particles and derivatives.

Materials	T_c (°C)	Grafting density (chains/nm^2)
VO_2	73.3	—
VO_2@PSS-12	76.9	n/a
VO_2@PSS-16	79.6	n/a
VO_2@PSS-20	79.5	n/a
VO_2@PSS-24	79.1	n/a
VO_2@PSS : PEDOT-12	79.6	6.51
VO_2@PSS : PEDOT-16	77.8	7.05
VO_2@PSS : PEDOT-20	77.8	5.35
VO_2@PSS : PEDOT-24	77.8	7.16
PSS	n/a	n/a
PSS : PEDOT	n/a	n/a

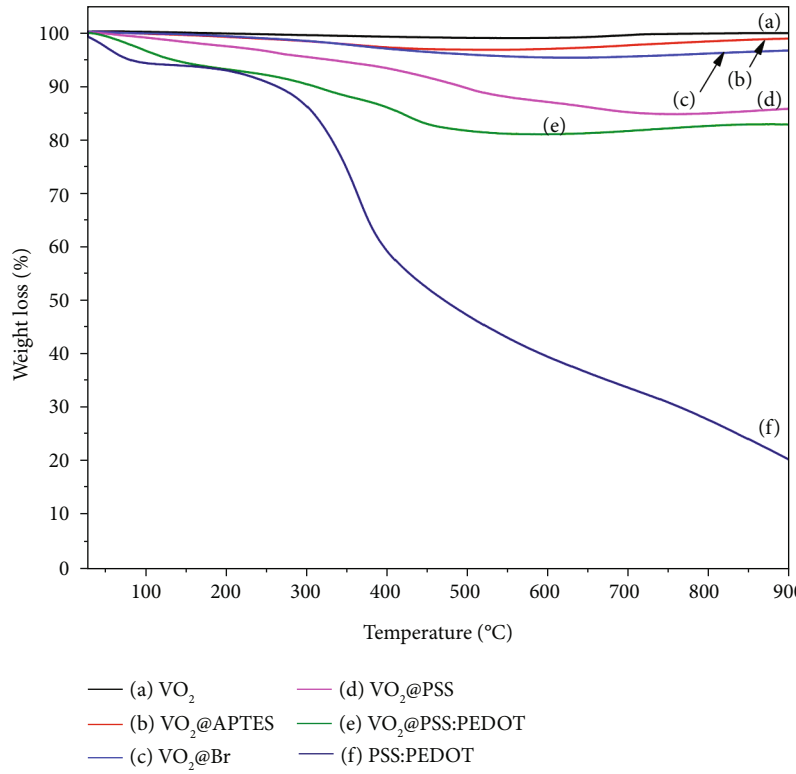

Figure 9: TGA thermograms of VO_2 particles and PSS : PEDOT polymer.

particles are in the range of 3000 and 5000 nm. Morphological changes of the VO_2 particle surface after grafting with polystyrene sulfonate (PSS) chains were noticed. This can be used as the evidence indicating the presence of polymer coating on VO_2 particles. In addition, results from dynamic light scattering analysis (DLS curves) of the various samples are presented in Figure 7. Some parameters derived from the DLS analysis, including size distribution and size at the maximum intensity of the major peaks (D_h) for those particles, are also summarized in Table 2. In this study, since the VO_2-based particles were agglomerated and exhibited multimodal characteristics, no further attempts were made to determine the average size of the particles from the above techniques.

3.2. Thermal Properties of the Modified VO_2 Particles. Figure 8 shows DSC thermograms of the various types of VO_2 particles. An endothermic peak at 73°C can be observed from the thermogram of the neat VO_2. This refers to the critical transition temperature (T_c) of the monoclinic VO_2. The critical transition temperature (T_c) of grafted products (VO_2@PSS) shifted slightly to a higher temperature ranging between 76.9°C and 79.6°C (Table 3). This was most likely due to the presence of grafting polymer chains on the surface of the VO_2 particles, which affected the heat transfer and the onset of the phase transition temperature of the VO_2. After polymerization with the EDOT monomer, the critical transition temperature of the products (VO_2@PSS : PEDOT) still existed and those ranged between 77.8°C and 79.6°C.

Notably, after grafting of the VO_2 particles with PPS chains, an additional peak, centered at around 164-174°C, was observed. This peak also existed in a thermogram of PSS homopolymer (see also the inset in Figure 8). The transition temperature of this peak is much lower than the melting peak of PSS, which is around 450°C [33]. Interestingly, after running a second heating DSC scan, the above peaks disappeared. The similar effect was observed by Zhou et al. in a study on temperature-dependent microstructure of PEDOT/PSS films [34]. Accordingly, the above peak was described to the release of water during heating. Finally, after polymerization of EDOT monomer, the position of this peak shifted to the lower temperatures (ranging between 145.1 and 147.2°C, see also Table 3). A similar trend was noticed in the case of PSS homopolymer and PSS/PEDOT blend systems (which were polymerized without the presence of VO_2 particles). In our opinion, the above changes were related to changes in polarity and hydrophilicity on the surface of VO_2@PSS particles after coupling with the polymerized PEDOT chains.

Figure 9 shows TGA thermograms of the synthesized PSS : PEDOT and various types of VO_2 particles. The thermogram of the PSS : PEDOT shows three major transitions including an initial weight loss, which occurred at a temperature below 110°C, owing to the loss of some absorbed moisture. The second transition occurred over temperatures ranging between 250°C and 400°C, and that was attributed to the elimination of the sulfonate groups ($-SO_3$) attached to the styrene rings in the PSS molecules [35, 36]. The third

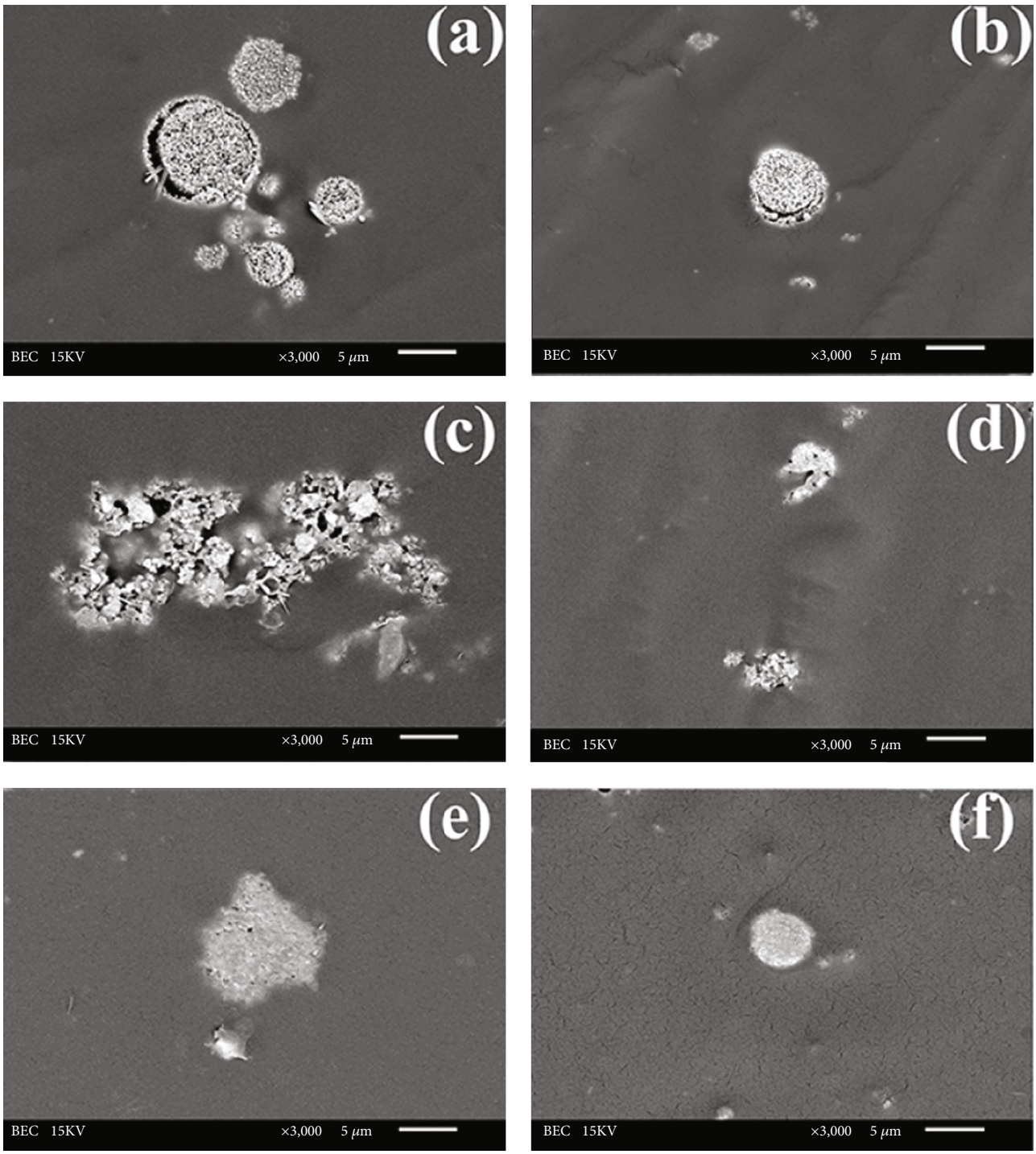

Figure 10: Backscattered electron SEM images of polymer composite films containing different types and concentrations of VO_2 particles: (a) acrylic/VO_2 (1.0 wt%), (b) acrylic/VO_2 (1.5 wt%), (c) acrylic/VO_2@PSS : PEDOT-12 (1.0 wt%), (d) acrylic/VO_2@PSS : PEDOT-12 (1.5 wt%), (e) acrylic/VO_2@PSS : PEDOT-24 (1.0 wt%), and (f) acrylic/VO_2@PSS : PEDOT-24 (1.5 wt%).

transition occurred over temperatures ranging between 300°C and 550°C, and that was attributed to the degradation of the polymers (PEDOT [28] and PSS [32, 37] chains).

By contrast, the neat VO_2 particles were thermally stable up to 900°C. TGA thermograms of the intermediates, which included VO_2 particles functionalized with silane (VO_2@APTES) and VO_2@APETS treated with the BIBB initiator (the so called VO_2@Br), show a gradual weight loss transition over temperatures between 120 and 600°C. This can be ascribed to the loss of functional groups on the surface of the chemically modified VO_2 particles. Finally, after grafting with PSS followed by coupling with PEDOT molecules, all these transitions can be observed from the TGA thermograms of the final product (VO_2@PSS : PEDOT).

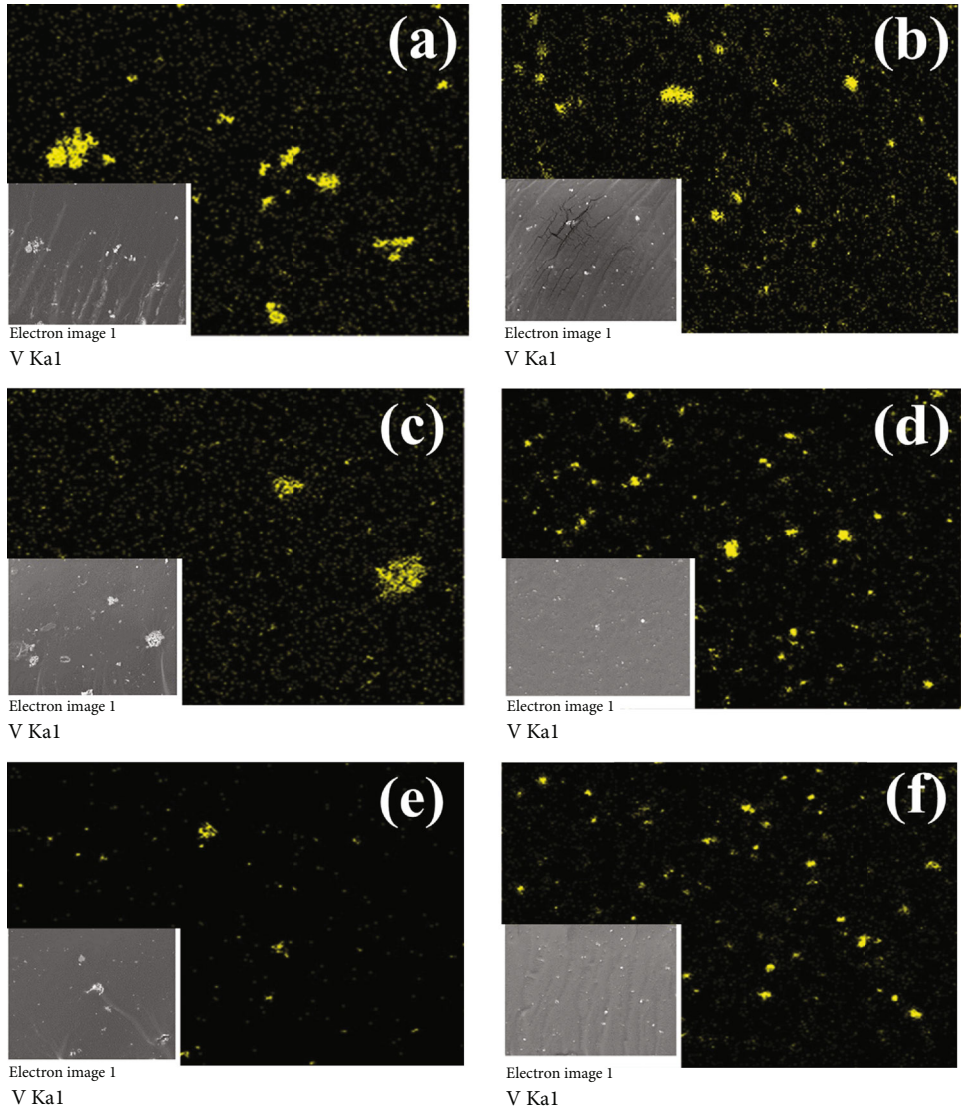

FIGURE 11: Electron images and EDX dot maps of polymer films containing different types and concentrations of VO_2 particles: (a) acrylic/VO_2 (1.0 wt%), (b) acrylic/VO_2 (1.5 wt%), (c) acrylic/VO_2@PSS : PEDOT-12 (1.0 wt%), (d) acrylic/VO_2@PSS : PEDOT-12 (1.5 wt%), (e) acrylic/VO_2@PSS : PEDOT-24 (1.0 wt%), and (f) acrylic/VO_2@PSS : PEDOT-24 (1.5 wt%).

In this regard, the grafting density of the final products was determined using equation (1), and the results are summarized in Table 3. Notably, grafting density values ranging from 5.35 to 7.16 chains/mm^2 were obtained, and the values changed with the polymerization time in a nonlinear fashion. In our opinion, the above effect can be ascribed to the nature of the SI-ATRP mechanism. The longer the reaction time, the greater the monomer conversion [38]. This led to the higher degree of particles covered by grafting chains [39]. Moreover, the mechanism of SI-ATRP is basically a kind of controlled free radical polymerization, which means that the length of the polymerized chains also gradually increased with the reaction time [40]. In this regard, it was possible that both parameters contributed to the number of chains per area (the grafting density values) of the VO_2@PSS : PEDOT reported in this study. It is also worth mentioning that the grafting density values of the modified VO_2 particles in this study are relatively high compared to those of the Fe_3O_4 nanoparticles grafted with poly(methyl methacrylate) chains, reported by Babu and Raghavachari [26]. In our opinion, the discrepancy was attributed to the different sizes and surface areas of the particles used. Specifically, the surface area of VO_2 (15.9887 m^2/g) is relatively low compared to that of the Fe_3O_4 nanoparticle (115 m^2/g).

3.3. Morphological, Optical, and Thermochromic Properties of Polymer/VO_2 Films. Figure 10 shows SEM images of acrylic polymer composite films loaded with 1 wt% of different types of VO_2 particles. It can be clearly seen that voids or gaps in the interface between particles and the polymer matrix disappeared after the neat VO_2 particles were replaced by the VO_2@PSS : PEDOT particles. This indicates that the state of compatibility between the acrylic polymer

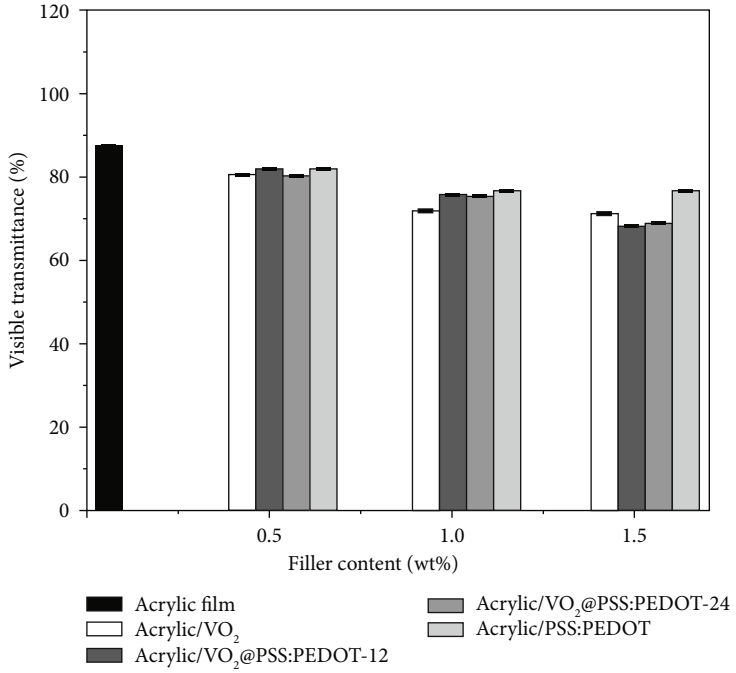

Figure 12: Percentage visible light transmittance of acrylic composite films containing different types and concentrations of VO_2-based particles.

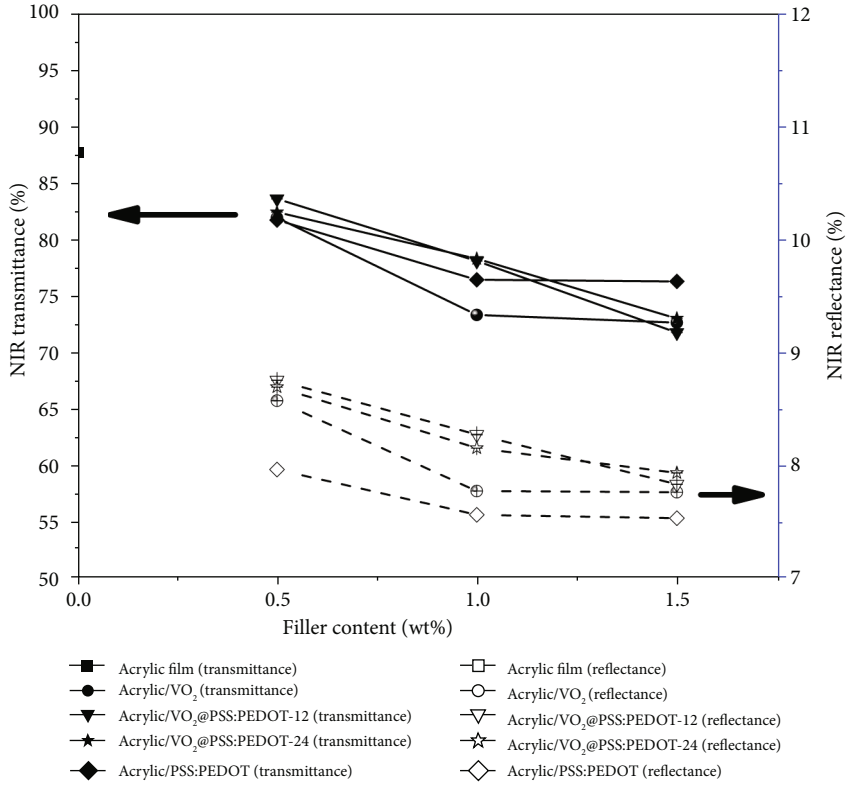

Figure 13: Percentages of near infrared (NIR) transmittance and NIR reflectance of acrylic composite films containing different types and concentrations of VO_2-based particles.

and the grafted VO_2 improved. In addition, from the EDX dot maps (Figure 11), greater dispersion of the particles in the acrylic polymer matrix can also be noticed.

The optical properties of acrylic film containing different types and concentrations of VO_2 particles are presented in Figures 12 and 13. The percentage visible light transmittance

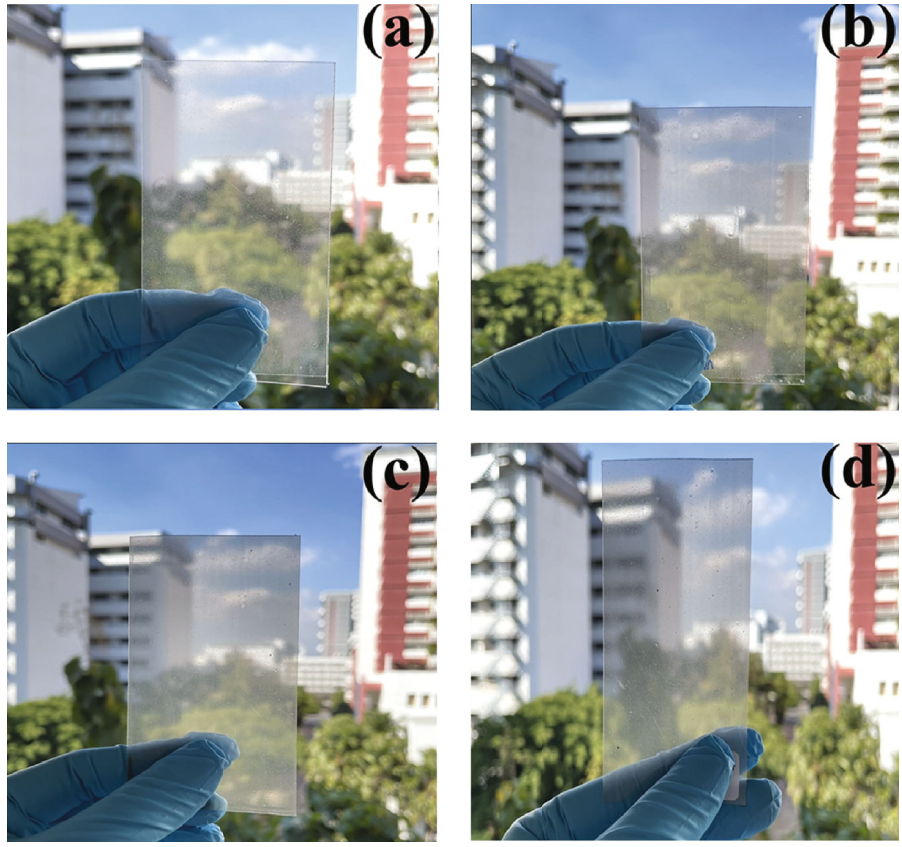

FIGURE 14: Photographs of substrates coated with polymer films containing different types of VO_2 particles (1 wt% loading): (a) the neat acrylic film, (b) acrylic/VO_2, (c) acrylic/VO_2@PSS : PEDOT-12, and (d) acrylic/VO_2@PSS : PEDOT-24.

(T_{Vis}) through the acrylic polymer film dropped from 87% to 81-82%, after loading with 0.5% of the neat VO_2 particles. The transmittance values tended to decrease with increasing concentration of VO_2 particles. A similar trend is also observed for the polymer composite films containing the modified VO_2 (VO_2@PSS : PEDOT) particles. The percentage visible light transmittance (T_{Vis}, %) of each composite film decreased to the lowest values, ranging between 68% and 71%, when the polymer was loaded with 1.5 wt% of VO_2-based particles. These values became lower than those of some existing commercial products such as heat control window films [41]. Therefore, in this study, no further attempts were made to increase the concentration of VO_2 particles beyond 1.5 wt%.

Figure 14 shows the appearance of polymer composite films containing different types of VO_2 particles. The optical transparency of these films can hardly be differentiated by the naked eye, probably because the percentage loading of the particles is only 1.0 wt%. However, consideration of the percentage transmittance (Figure 12) reveals that a T_{Vis} value above 75% of the composite films could be reached when the neat VO_2 particles were replaced with VO_2@PSS : PEDOT particles. Again, the improvement could be attributed to better dispersion of the particles after surface modification. However, as the concentration of VO_2@PSS : PEDOT was further increased to 1.5 wt%, the T_{Vis} values of the composite film decreased again and became closer to the T_{Vis} value of the acrylic/neat VO_2 film. This was due to more agglomeration of the modified VO_2 particles at higher loading (Figure 11). Interestingly, by using PSS and PEDOT (polymerized without the presence of VO_2 particles) as fillers, the transparency of the acrylic film also decreased. This was probably due to poor miscibility between the acrylic polymer and PSS/PEDOT. Moreover, the actual content of PSS/PEDOT chains loaded into the acrylic film was 1.0 wt%, which is much higher (about 10 times) than the actual weight of the PSS : PEDOT grafted onto the modified VO_2 particles. These factors contributed to the decrease in transparency. Nevertheless, the T_{Vis} values of the acrylic polymer/VO_2@PSS : PEDOT composite films in this study are much greater than those of the EVA/VO_2@PE composites in our earlier report [12], provided that the same volume of VO_2 particles were loaded (1.0 wt%) (see Table 4). In our opinion, the discrepancy could be attributed to several factors, including the fact that different polymers and mixing processes were used. Hereafter, acrylic-based emulsion was used, and the mixing was carried out via a solution process. By contrast, EVA pellets were compounded with additives and VO_2 particles via an extrusion process under shear force and heat. In this regard, a different state of dispersion of the particles in the polymer matrices can be obtained. Besides this, the PSS and PEDOT grafting chains used in this study are intrinsically transparent. This feature contributed significantly to the greater T_{Vis} of the acrylic film (Table 4). The above effect

Table 4: Comparison of optical properties of various polymer composite films containing different types of VO_2 particles (1.0 wt% loading).

Samples	T_{Vis} (%)	T_{NIR} (%)	Refs
EVA film (solution mixing)	89.95 (±0.54)	n/a	[1]
EVA film (melt mixing)	85.98 (±0.97)	n/a	[1]
EVA/VO_2 (solution mixing)	73.73 (±0.56)	n/a	[1]
EVA/VO_2 (melt mixing)	31.60 (±0.73)	n/a	[1]
EVA film (melt mixing)	90.20 (±0.83)	89.35 (±0.54)	[12]
EVA/VO_2 (melt mixing)	43.21 (±2.17)	42.48 (±2.12)	[12]
EVA/VO_2@PE (melt mixing)	41.91 (±1.28)	44.82 (±1.34)	[12]
Acrylic film	87.55 (±0.0049)	87.73 (±0.0030)	This study
Acrylic/VO_2	71.84 (±0.0027)	73.29 (±0.0049)	This study
Acrylic/VO_2@PSS : PEDOT-12	75.81 (±0.0020)	78.07 (±0.0.0025)	This study

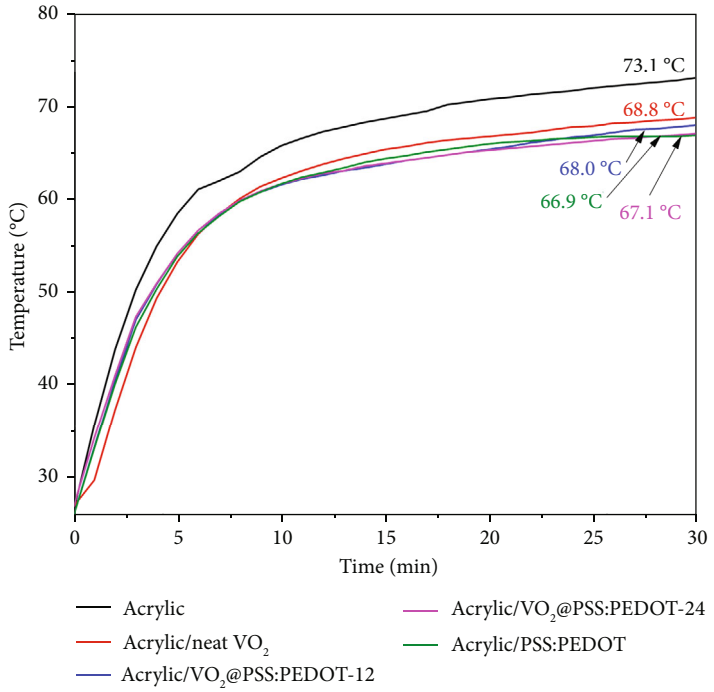

Figure 15: Change in temperature inside the model house installed with glass windows which were coated with various acrylic/VO_2 (1.0 wt%) composite films.

was not the case for the VO_2 coated with polyethylene, which is opaque.

Apart from the optical transparency, the percentage NIR transmittance (T_{NIR}) through the polymer films also decreased when the VO_2 particles were loaded. The higher the concentration of modified VO_2 particles, the lower the T_{NIR} values. However, the percentage NIR reflectance (R_{NIR}) of these films did not increase, regardless of the type of concentration of VO_2-based particles. It is important to remember that the UV/Vis/NIR spectroscopy test was carried out at ambient temperature, which is below the T_c of the VO_2 particles. Therefore, the metal oxide particles remained in a monoclinic phase, VO_2(M), which is incapable of reflecting the transmission of NIR radiation effectively. In this regard, the decrease in percentage NIR transmittance through the acrylic/VO_2@PSS : PEDOT composite film could be attributed uniquely to other factors including a light-scattering effect and the presence of PSS and PEDOT chains on the surface of the modified VO_2 particles. In addition, a significant amount of the NIR radiation was absorbed by metal oxide particles in the polymer composite films. A similar effect was also observed in the PVC/VO_2 composites [42], and that influenced the thermal stability and durability of the composite films.

The heat shielding properties of the composite films containing VO_2 particles, however, began to appear and became remarkable when these samples were tested in a model house, installed with thermocouples and an infrared lamp. It is worth mentioning that when the lamp was turned on, the actual temperature in front of the model house was equal to 85°C, which is above the T_c of the VO_2 particles. In this regard, it was possible that the monoclinic crystal structure

of the VO_2 particles changed to the rutile phase, which is thermochromic and capable of exhibiting NIR shielding properties. From Figure 15, the temperature of the normal acrylic polymer film (without VO_2 particles) increased steadily with time and reached a plateau at 85°C, after 30 min. However, when VO_2 particles were loaded into the acrylic polymer film, the temperature, after reaching equilibrium, decreased by 4.3°C.

Finally, when the neat VO_2 particles were replaced by the modified VO_2 particles, similar trends still existed. The final temperature after equilibrium of the system equipped with these films was also slightly lower than that installed with the neat VO_2/acrylic film. However, the differences were not obvious. Since the critical transition temperature of VO_2 increased slightly after the surface modifications (see Table 3), it was possible that the phase transition of the modified VO_2 particles did not occur completely and so the NIR shielding efficacy of the materials was not fully exhibited. In addition, further work has yet to be carried out to optimize the grafting density and percentage loading of modified VO_2 particles in this system.

4. Conclusions

Vanadium dioxide particles grafted with polystyrene sulfonate/poly(3,4-ethylenedioxythiophene) (VO_2@PSS:PEDOT) were successfully prepared via surface functionalization and surface-initiated atom transfer radical polymerization. The thermochromic behaviors of the modified VO_2 particles were observed with phase transition temperatures ranging between 78 and 79°C. Window films made from the acrylic/VO_2@PSS:PEDOT (1.0 wt%) were capable of reducing the temperature inside a model house, of up to 5-6°C, compared with the control system (the acrylic coating without any particles). Overall, this study has demonstrated that it is possible to improve the dispersion of VO_2-based particles in acrylic polymer by grafting with PSS:PEDOT chains.

Data Availability

The data concerning the detailed synthesis procedure for preparation of various VO_2-based particles are described and reported within the supplementary information file. Additional data used to support the findings of this study are available from the corresponding author upon request.

Conflicts of Interest

The authors declare that they have no conflicts of interest.

Acknowledgments

Ms. Srirodpai is sincerely grateful to the scholarship provided by King Mongkut's University of Technology Thonburi through the "KMUTT 55th Anniversary Commemorative Fund (Petchra Pra Jom Klao Doctoral Scholarship)." Special thanks go to Mr. Alongkorn Nukulpakdi, from the RPSC Chemicals Co. Ltd., for providing the acrylic emulsion used as a binder for making polymer films in this work.

Supplementary Materials

Detailed synthesis procedures of the various vanadium dioxide-based particles. *(Supplementary Materials)*

References

[1] O. Srirodpai, J. Wootthikanokkhan, S. Nawalertpanya, K. Yuwawech, and V. Meeyoo, "Preparation, Characterization and Thermo-Chromic Properties of EVA/VO2 Laminate Films for Smart Window Applications and Energy Efficiency in Building," *Materials*, vol. 10, no. 1, p. 53, 2017.

[2] M. Kamalisarvestani, R. Saidur, S. Mekhilef, and Javadi, "Performance, materials and coating technologies of thermochromic thin films on smart windows," *Renewable and Sustainable Energy Reviews*, vol. 26, pp. 353–364, 2013.

[3] Y. Dang, D. Wang, X. Zhang, L. Ren, B. Li, and J. Liu, "Structure and thermochromic properties of Mo-doped VO2 thin films deposited by sol–gel method," *Inorganic and Nano-Metal Chemistry*, vol. 49, no. 4, pp. 120–125, 2019.

[4] C. Batista, R. M. Ribeiro, and V. Teixeira, "Synthesis and characterization of VO_2-based thermochromic thin films for energy-efficient windows," *Nanoscale Research Letters*, vol. 6, no. 1, pp. 301–308, 2011.

[5] P. Kiri, M. E. A. Warwick, I. Ridley, and R. Binions, "Fluorine doped vanadium dioxide thin films for smart windows," *Thin Solid Films*, vol. 520, no. 4, pp. 1363–1366, 2011.

[6] Y. Cui, Y. Ke, C. Liu et al., "Thermochromic VO2 for Energy-Efficient Smart Windows," *Joule*, vol. 2, pp. 1707–1746, 2018.

[7] T. Chang, X. Cao, S. Bao, S. Ji, H. Luo, and P. Jin, "Review on thermochromic vanadium dioxide based smart coatings: from lab to commercial application," *Advanced Manufacturing*, vol. 6, no. 1, pp. 1–19, 2018.

[8] H. Ho, Y. Lai, K. Chen, T. D. Dao, C. H. Hsueh, and T. Nagao, "High quality thermochromic VO_2 films prepared by magnetron sputtering using V_2O_5 target with in situ annealing," *Applied Surface Science*, vol. 495, article 143436, 2019.

[9] D. Malarde, M. J. Powell, R. Quesada-Cabrera et al., "Optimized atmospheric-pressure chemical vapor deposition thermochromic VO_2 thin films for intelligent window applications," *ACS Omega*, vol. 2, no. 3, pp. 1040–1046, 2017.

[10] D. Bhardwaj, A. Goswami, and A. M. Umarji, "Synthesis of phase pure vanadium dioxide (VO_2) thin film by reactive pulsed laser deposition," *Japanese Journal of Applied Physics*, vol. 124, no. 13, article 135301, 2018.

[11] R. Lopez, L. A. Boatner, T. E. Haynes, L. C. Feldman, and R. F. Haglund, "Synthesis and characterization of size-controlled vanadium dioxide nanocrystals in a fused silica matrix," *Japanese Journal of Applied Physics*, vol. 92, no. 7, pp. 4031–4036, 2002.

[12] O. Srirodpai, J. Wootthikanokkhan, and S. J. Nawalertpanya, "Preparation, characterizations and oxidation stability of polyethylene coated nanocrystalline VO_2 particles and the thermochromic performance of EVA/VO_2@PE composite film," *Nanoscience and Nanotechnology*, vol. 19, no. 6, pp. 3356–3366, 2019.

[13] Y. Gao, S. Wang, H. Luo et al., "Enhanced chemical stability of VO_2 nanoparticles by the formation of SiO_2/VO_2 core/shell structures and the application to transparent and flexible VO_2-based composite foils with excellent thermochromic properties for solar heat control," *Energy & Environmental Science*, vol. 5, no. 3, pp. 6104–6110, 2012.

[14] K. Tong, R. Li, J. Zhu et al., "Preparation of VO_2/Al-O core-shell structure with enhanced weathering resistance for smart window," *Ceramics International*, vol. 43, no. 5, pp. 4055–4061, 2017.

[15] Y. Zhou, Y. Cai, X. Hu, and Y. J. Long, "VO_2/hydrogel hybrid nanothermochromic material with ultra-high solar modulation and luminous transmission," *Journal of Materials Chemistry A*, vol. 3, no. 3, pp. 1121–1126, 2015.

[16] J. W. Youn, S. J. Lee, K. S. Kim, J. W. Han, and D. U. Kim, "A study on the change of VO_2 thin-film coating behavior according to the droplet size using ultrasonic spray," *Applied Physics A: Materials Science & Processing*, vol. 127, no. 4, pp. 183–193, 2021.

[17] S. Mallakpour and M. Madani, "A review of current coupling agents for modification of metal oxide nanoparticles," *Progress in Organic Coating*, vol. 86, pp. 194–207, 2015.

[18] S. K. Kumar, N. Jouault, B. Benicewicz, and T. Neely, "Nanocomposites with polymer grafted nanoparticles," *Macromolecules*, vol. 46, no. 9, pp. 3199–3214, 2013.

[19] Y. Li, S. Ji, Y. Gao, H. Luo, and M. Kanehira, "Core-shell VO_2@TiO_2 nanorods that combine thermochromic and photocatalytic properties for application as energy-saving smart coatings," *Scientific Reports*, vol. 3, no. 1, pp. 1370–1388, 2013.

[20] W. Li, S. Ji, G. Sun, Y. Ma, H. Guo, and P. Jin, "Novel VO_2(M)–ZnO heterostructured dandelions with combined thermochromic and photocatalytic properties for application in smart coatings," *New Journal of Chemistry*, vol. 40, no. 3, pp. 2592–2600, 2016.

[21] H. J. Yoon, S. Y. Jeong, S. Lee, G. Shin, and K. H. Choi, "Near infrared shielding properties of PEDOT: PSS with different additives," in *4th Int. Conf., Biological and Environmental Engineering*, pp. 35–39, Phuket, Thailand, 2012.

[22] S. Im, C. Park, W. Cho, J. Kim, M. Jeong, and J. Kim, "Synthesis of solution-stable PEDOT-coated sulfonated polystyrene copolymer PEDOT:P(SS-co-St) particles for all-organic NIR-shielding films," *Coatings*, vol. 9, no. 3, pp. 151–161, 2019.

[23] K. Yoshida, S. Nagaoka, M. Horikawa, H. Noguchi, and H. Ihara, "Totally-organic near-infrared shielding materials by conductive cellulose nanofibers," *Thin Solid Films*, vol. 709, article 138221, 2020.

[24] C. Cai-Wan, C. Er-Chieh, Y. Shih-Chieh et al., "Facile preparation of WO3/PEDOT:PSS composite for inkjet printed electrochromic window and its performance for heat shielding," *Dyes and Pigments*, vol. 148, pp. 465–473, 2018.

[25] L. Janamphansang, J. Wootthikanokkhan, and S. Nawalertpanya, "Preparation of VO_2 nanoparticles with surface functionalization for thermochromic application," *Engineering Journal*, vol. 23, no. 5, pp. 205–215, 2019.

[26] K. Babu and D. Raghavachari, "Synthesis of Polymer Grafted Magnetite Nanoparticle with the Highest Grafting Density via Controlled Radical Polymerization," *Nanoscale Research Letters*, vol. 4, no. 9, pp. 1090–1102, 2009.

[27] P. Zhu, B. Liu, and L. Bao, "Preparation of double-coated TiO2 nanoparticles using an anchoring grafting method and investigation of the UV resistance of its reinforced PEI film," *Progress in Organic Coatings*, vol. 104, pp. 81–90, 2017.

[28] T. Wang, X. Zhang, D. Chen et al., "Preparation of a hybrid core–shell structured $BaTiO_3$@PEDOT nanocomposite and its applications in dielectric and electrode materials," *Applied Surface Science*, vol. 356, pp. 232–239, 2015.

[29] L. Ma, P. Luo, Y. He, L. Zhang, Y. Fan, and Z. Jiang, "Ultra-stable silica nanoparticles as nano-plugging additive for shale exploitation in harsh environments," *Nanomaterials*, vol. 9, no. 12, pp. 1683–1698, 2019.

[30] L. Latka, K. Goc, C. Kapusta, and S. Zapotoczny, "Enhanced thermal conductivity of polyamide-based nanocomposites containing graphene oxide sheets decorated with compatible polymer brushes," *Materials*, vol. 14, no. 4, p. 751, 2021.

[31] A. Farrukh, F. Ashraf, A. Kaltbeitzel et al., "Polymer brush functionalized SiO2nanoparticle based Nafion nanocomposites: a novel avenue to low-humidity proton conducting membranes," *Polymer Chemistry*, vol. 6, no. 31, pp. 5782–5789, 2015.

[32] X. Zhang, Y. Huang, L. Hu, C. Huang, H. Li, and Y. Zhang, "Synthesis and characterization of VO_2@poly(sodium styrene sulfonate)/polypyrrole using VO_2@PSS as a template," *Materials Express*, vol. 5, no. 4, pp. 351–358, 2015.

[33] C. Yang, K. Shin, and H. K. Jeong, "Thermal analysis of poly(-sodium 4-styrenesulfonate) intercalated graphite oxide composites," *Chemical Physics Letters*, vol. 517, no. 4-6, pp. 196–198, 2011.

[34] P. Balding, R. Borrelli, and P. S. Russo, "Physical properties of sodium poly(styrene sulfonate): comparison to incompletely sulfonated polystyrene," *Macromolecules*, vol. 55, no. 5, pp. 1747–1762, 2022.

[35] J. M. Slone, E. Napadensky, D. Crawford, and D. Suleiman, "Synthesis and mechanical properties of sulfonated block copolymers," *Annual Technical Conference - ANTEC, Conference Proceedings*, vol. 2, pp. 805–808, 2010.

[36] B. Smitha, S. Sridhar, and A. A. J. Khan, "Synthesis and characterization of proton conducting polymer membranes for fuel cells," *Journal of Membrane Science*, vol. 225, no. 1-2, pp. 63–76, 2003.

[37] X. Xiao, F. Lui, X. Z. Lui, and D. Zhu, "Effect of poly(sodium 4-styrene-sulfonate) on the crystal growth of hydroxyapatite prepared by hydrothermal method," *Materials Chemistry and Physics*, vol. 120, no. 2-3, pp. 603–607, 2010.

[38] P. Liu and Z. Su, "Surface-initiated atom transfer radical polymerization (SI-ATRP) of styrene from chitosan particles," *Materials Letters*, vol. 60, no. 9-10, pp. 1137–1139, 2006.

[39] S. Maeda, M. Fujita, N. Idota, K. Matsukawa, and Y. Sugahara, "Preparation of transparent bulk TiO_2/PMMA hybrids with improved refractive indices via an in situ polymerization process using TiO_2 nanoparticles bearing PMMA chains grown by surface-initiated atom transfer radical polymerization," *ACS Applied Materials & Interfaces*, vol. 8, no. 50, pp. 34762–34769, 2016.

[40] A. Neumann, H. Keul, and H. Höcker, "Atom transfer radical polymerization (ATRP) of styrene and methyl methacrylate with α,α-dichlorotoluene as initiator; a kinetic study," *Macromolecular Chemistry and Physics*, vol. 201, no. 9, pp. 980–984, 2000.

[41] Technical Data Sheet and PA Window Tint, "Specification for 3M control window film exterior prestige series," 2019, https://pawindowtint.com/wp-content/uploads/2021/11/3M-PrestigeX-20X-Spec.pdf.

[42] T. Sakuldeemeekiat, N. Luamsri, J. Wootthikanokkhan, and M. J. Phiriyawirut, "The effects of thermochromic pigments on optical, mechanical, and heat insulation properties of plasticized PVC window film," *Journal of Thermoplastic Composite Materials*, vol. 33, no. 9, pp. 1196–1216, 2020.